Thermal Spin Wave Noise as a Probe for the Dzyaloshinskii-Moriya Interaction

Aurore Finco,[1,*] Pawan Kumar,[1] Van Tuong Pham,[2,3] Joseba Urrestarazu-Larrañaga,[2] Rodrigo Guedas Garcia,[2] Maxime Rollo,[1] Olivier Boulle,[2] Joo-Von Kim,[4] and Vincent Jacques[1]

[1]*Laboratoire Charles Coulomb, Université de Montpellier, CNRS, 34095 Montpellier, France*

[2]*Université Grenoble Alpes, CNRS, CEA, SPINTEC, 38054 Grenoble, France*

[3]*IMEC, 3001 Leuven, Belgium*

[4]*Centre de Nanosciences et de Nanotechnologies, CNRS, Université Paris-Saclay, 91120 Palaiseau, France*

(Received 5 February 2025; accepted 26 August 2025; published 24 September 2025)

Interfacial Dzyaloshinskii-Moriya interaction (DMI) is a key ingredient in the stabilization of chiral magnetic states in thin films. Its sign and strength often determine crucial properties of magnetic objects, like their topology or how they can be manipulated with currents. A few experimental techniques are currently available to measure DMI quantitatively, based on the study of domain walls, spin waves, or spin-orbit torques. In this Letter, we propose a qualitative variant of spin wave methods. We rely on magnetic noise from confined thermal spin waves in domain walls and skyrmions in perpendicularly magnetized thin films, which we probe with scanning nitrogen-vacancy center relaxometry. We show both numerically and experimentally that the sign of the DMI can be inferred from the amplitude of the detected noise, which is affected by the nonreciprocity in the spin wave dispersion. Furthermore, we also demonstrate that the noise distribution around the contour of magnetic skyrmions reveals their Néel or Bloch nature, giving therefore also insight into the strength of DMI involved in their stabilization.

DOI: 10.1103/dvbq-9z5f

Magnetic noise provides valuable information about systems in which incoherent or thermal magnetic excitations, as well as fluctuating spins, play a crucial role [1]. For example, noise spectroscopy can provide access to electron and hole spin dynamics in semiconductors [2,3], properties of nanoparticles [4–7], information on magnetic materials close to a phase transition [8], the detection of thermal spin waves [9,10], and spin transport phenomena [11]. Quantum sensors like nitrogen-vacancy (NV) centers in diamond are especially useful to investigate these noise-related phenomena owing to their high sensitivity to their environment, whose fluctuations modify their spin relaxation properties [12]. Integrating an NV sensor into an atomic force microscope combines high sensitivity noise sensing with nanoscale spatial resolution [13]. This approach, referred to as scanning relaxometry, allows the realization of electrical conductivity maps [14] or the investigation of magnetic textures, in particular, in low-moment materials like antiferromagnets [15].

In this Letter, we demonstrate how scanning relaxometry using NV centers can be harnessed to characterize the *handedness* of chiral spin textures, which in thin ferromagnetic films are governed by the sign and strength of the Dzyaloshinskii-Moriya interaction (DMI) [16,17]. It is known that thermal spin waves within textures like domain walls lie within the GHz range, which affects the longitudinal spin relaxation time T_1 of the NV center [18]. The core idea of this Letter is that the nonreciprocal propagation of these spin waves, resulting from the nearest-neighbor DMI, also gives rise to different noise profiles above and below the film, from which information about the handedness of the spin textures can be deduced.

We first illustrate the concept by considering an ultrathin ferromagnetic film in contact with a heavy-metal underlayer, which induces an interfacial DMI [19,20]. This form of the interaction favors spin spirals propagating in the film plane [21], which translates into an asymmetric dispersion relation for spin waves in the Damon-Eshbach geometry for in-plane magnetized films [22–24], but does not affect perpendicularly magnetized systems in which propagation remains isotropic. This effect has been probed in Brillouin light scattering experiments in which the asymmetry in the spin wave dispersion relation [25] can be measured to quantify the nearest-neighbor interfacial DMI. This technique is however only applicable to in-plane magnetized layers. For a perpendicularly magnetized film in a multidomain state [Fig. 1(a)], both reciprocal and nonreciprocal propagation are possible depending on where the propagation takes place. Within the domains, along the line indicated by x_d in Fig. 1(a), the dispersion is reciprocal as shown in Fig. 1(b). Along a 180° Néel domain wall at the position x_w, on the other hand, the dispersion relation is strongly nonreciprocal with a narrow frequency gap as shown in Fig. 1(c), where both the DMI and dipolar interactions contribute to the asymmetry [26,27].

*Contact author: aurore.finco@umontpellier.fr

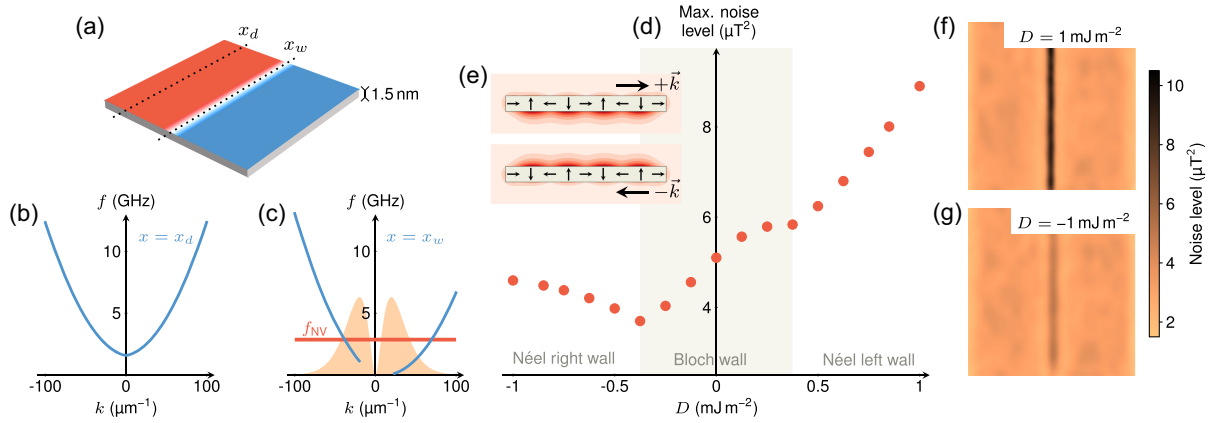

FIG. 1. (a) Sketch of the considered out-of-plane magnetized Co layer. (b),(c) Calculated spin wave dispersion in the Co layer with $D = 1.0$ mJ m^{-2}, in (b) the domains (at $x = x_d$), and in (c) the domain walls (at $x = x_w$). The orange shading in (c) represents the k-filtering function at a distance of 50 nm. No data are shown for small k in the domain wall because a perfectly straight wall is unstable under these conditions. (d) Calculated maximal noise level at 2.87 GHz and at 50 nm from the film surface, when varying the DMI constant D. (e) Sketch of the stray field produced by Halbach arrays. (f),(g) Calculated noise map 50 nm above the film, for $D = \pm 1.0$ mJ m^{-2}.

The degree of asymmetry increases with D, as shown in Fig. S2 of Supplemental Material (SM) [28].

Our objective is then to probe the magnetic noise produced by thermal spin waves inside such a domain wall using a single NV center placed above the magnetic film. Previous studies on synthetic antiferromagnets [18] have shown how the resulting fluctuating magnetic fields shorten the longitudinal spin relaxation time T_1, leading to a reduction of the photoluminescence (PL) signal emitted by the NV center [33]. This sensing method effectively filters the probed noise twice: it is frequency-filtered as only the frequency components around the magnetic resonance frequencies of the NV center [$f_{\mathrm{NV}} \sim 2.87$ GHz at zero field, depicted by the red line in Fig. 1(c)], can enhance its relaxation, and it is wave-vector-filtered as the NV sensitivity to fluctuations is broadly peaked around $(1/d_{\mathrm{NV}})$, where d_{NV} is the distance between the NV center and the magnetic film. This filter function $ke^{-2kd_{\mathrm{NV}}}(1 - e^{-2kt})$ [9,10] is represented by the orange shading in Fig. 1(c). This double filtering, combined with the asymmetric dispersion relation, means that the NV center is mostly sensitive to noise arising from modes with a given wave vector direction determined by the sign of D.

Note that no significant stray fields are expected from propagating spin waves in out-of-plane uniformly magnetized thin films; most reports to date in the literature [9,10,34–40], except Ref. [18], concern in-plane magnetized materials. In a perpendicularly magnetized film, the dynamic magnetization components of the propagating spin waves lie in the film plane, with $\vec{k}$ orthogonal to the static magnetization. These fluctuations do not produce surface or volume magnetic charges, so no fluctuating stray fields are expected.

Figure 1(d) displays the expected noise level detectable by an NV center, positioned above a 180° domain wall at $d_{\mathrm{NV}} = 50$ nm from the film surface, as a function of D, and thus also of the internal structure of the walls. These levels were computed following the method described in Refs. [18,28]. Notably, we observe a significant difference in noise levels for left- and right-handed Néel walls. The conjunction of two phenomena gives rise to this effect. First, spin waves with opposite wave vectors about a static in-plane magnetization produce magnetic stray fields mainly above or below the film [41]. This can be understood by drawing an analogy between the magnetization fluctuations of the spin wave with the magnetic order within a Halbach array [Fig. 1(e)]. The stray field generated by the arrangement of the in-plane magnetization compensates the contribution from the out-of-plane component on one side of the film but reinforces it on the other side, resulting in a one-sided flux magnetization configuration [42]. Reversing the handedness of the Halbach array results in the dominant flux being generated on the opposite film surface. Second, the DMI-induced nonreciprocity, $\omega(k) \neq \omega(-k)$, means that thermal populations of modes with opposite wave vector are unequal, i.e., $n(k) \neq n(-k)$ with $n(k) \simeq k_B T/\hbar\omega(k)$ in the long wavelength limit. This population imbalance grows as the dispersion becomes more asymmetric with the strength of D, which is reflected in the variation of the noise level. The noise maps in Figs. 1(f) and 1(g) show the expected signal above Néel left and right domain walls, with $D = \pm 1.0$ mJ m^{-2}, at a distance of 50 nm from the film. A stronger noise contrast is expected for the Néel left wall, offering us the ability to determine the handedness of domain walls with this approach. We add that previous work has reported the possibility to probe the chirality of the spin waves themselves [43] with NV center relaxometry, through the handedness of their stray field. This requires one to address

separately the two electronic spin transitions of the NV center, which is however not necessary in our case to find the sign of D.

We now turn to the experimental investigation of this effect using scanning NV center microscopy. We will measure static stray field maps by monitoring the Zeeman shift of the NV center magnetic resonance, and probe spin wave noise through the acceleration of the NV center relaxation and the subsequent PL decrease. Instead of the ferromagnetic layer discussed above, we study synthetic antiferromagnets (SAFs) comprising two Co layers coupled antiferromagnetically through a Ru/Pt spacer [29,44]. This choice is motivated by the low static stray field generated by the antiparallel magnetizations, i.e., < 1 mT measured at the NV center position, in contrast to 15 mT at 60 nm above a domain wall in a single 1.5 nm-thick Co layer. Moreover, the stray field distribution from a ferromagnet possesses a strong off-axis component with respect to the NV axis, which corresponds to the direction joining the nitrogen atom and the vacancy. This off-axis field leads to a mixing of the NV center spin states, and a drop of the emitted PL [45]. This drop would further compound the PL decrease induced by the shortening of T_1 by magnetic noise. Using a SAF in our experiment therefore allows us to avoid this unwanted effect and to focus solely on the response of the NV center to thermal spin wave noise. Nevertheless, experiments on a single Co layer were also performed (Fig. S1 [28]) and agree with our theoretical predictions. All our measurements are achieved under the application of a few mT bias field used to separate the magnetic resonances of the NV center during quantitative measurements, but not affecting the magnetic texture or the noise detection, as the noise has a broad frequency spectrum.

We perform the first experiment on a SAF grown on Si/SiO_2, with the composition indicated in Fig. 2(a). We measure the PL emitted by the NV center as the tip is scanned over the sample surface at a distance $d_{NV} = 62 \pm 5$ nm from the top Co layer (details of the tip calibration are given in Ref. [28]). As in Ref. [18] we observe a drop of PL above the domain walls, owing to the enhancement of the NV spin relaxation by the magnetic noise associated with spin waves localized within the wall. This enhancement of the relaxation rate is shown in Figs. 2(c) and 2(d), which compare measurements of T_1 taken above a domain and a wall, respectively. The measurement sequence used is shown in Fig. 2(b) and details are provided in Ref. [28]. The error bars on the data point are obtained assuming Poissonian noise on the PL signal, and the values of T_1 are extracted from a fit to an exponential decay. In this sample, the wall type is expected to be left-handed Néel as the DMI arises from the Pt/Co interface, and was measured to be $D = 0.62 \pm 0.24$ mJ m^{-2} [29]. We are therefore in the favorable case for detection, with a strong noise contribution above the film.

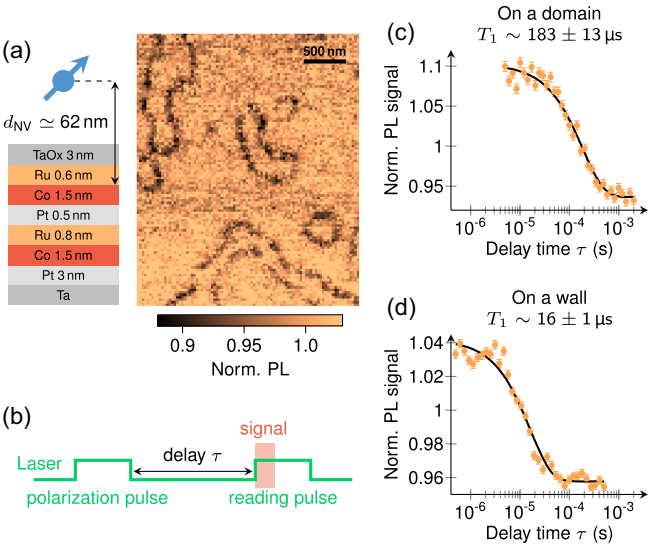

FIG. 2. (a) Noise map of the SAF sketched on the left, measured with scanning NV center microscopy and revealing the presence of domain walls. Accumulation time per pixel 50 ms. (b) Sketch of the measurement sequence to obtain relaxation time curves. (c),(d) Relaxation time curves measured above a domain (c) or above a wall (d), showing a strong decrease of T_1 above the wall. Black lines are fits to an exponential decay.

Figure 3 presents a similar experiment performed on an inverted stack, such that the sign of D is reversed. We first attempted growing the multilayer stack in reverse order on Si/SiO_2, but this resulted in weak perpendicular anisotropy in the Co layers such that it was not possible to stabilize perpendicularly magnetized domains. Instead, we substituted the Si/SiO_2 substrate for an about 20 nm-thick SiN membrane, keeping the same growth order, and performed the scanning NV microscopy on the back of the sample through the membrane. To compensate for the thickness of the membrane, we use another diamond probe with an NV center closer to the surface, resulting in a net distance $d_{NV} = 72 \pm 5$ nm. The noise map obtained and shown in Fig. 3(a) is blank, in contrast to the clear 10% decrease of PL above the walls in Fig. 2(a). Figure 3(b) displays the static magnetic stray field measured simultaneously with the noise map in panel (a) and reveals the presence of domain walls in this area.

In order to investigate further this sample, we again measured T_1 above a uniformly magnetized region and a domain wall [Figs. 3(c) and 3(d)]. No significant difference is seen between these two experiments, which suggests that the detectable noise level is smaller for right-handed than left-handed Néel walls as predicted by our model. Our measurements performed on a single Co layer, with an identical diamond probe and identical d_{NV} for both chiralities, also support this finding (Fig. S1 [28]), albeit with lower-quality measurements related to the stronger stray fields. We have thus demonstrated that the noise level above Néel walls is correlated to their handedness in

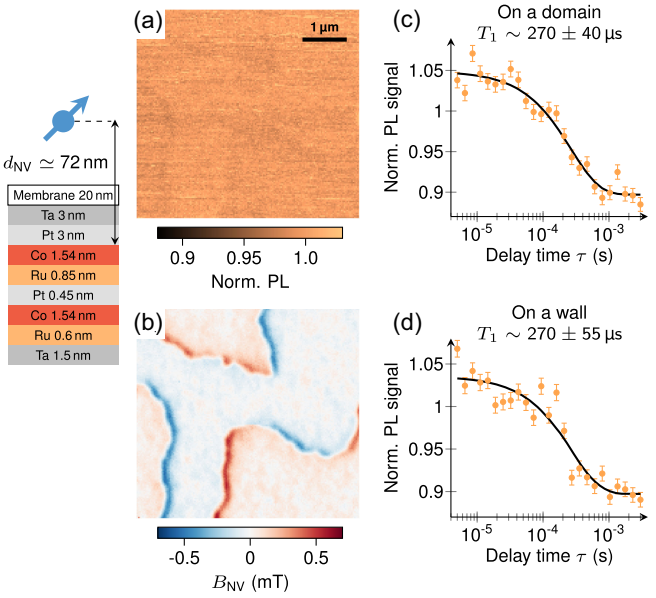

FIG. 3. (a) Thermal noise map measurement on a reversed stack grown on a membrane. (b) Stray field map measured simultaneously with (b), showing the position of the domain walls. Accumulation time per pixel 1.5 s, the PL level map (a) is extracted from the optically detected magnetic resonance spectra at each pixel. (c),(d) Relaxation time curves measured above a domain (b) or above a domain wall (c). Black lines are fits to an exponential decay.

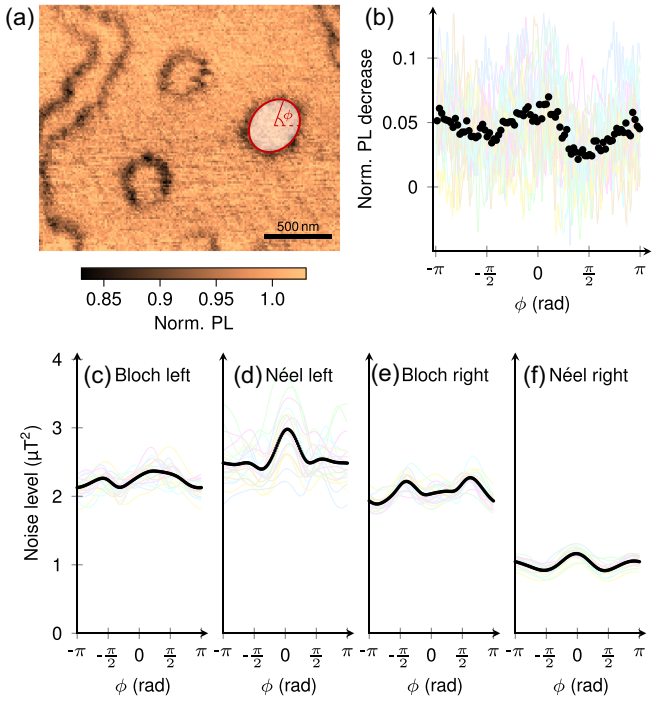

FIG. 4. (a) Noise map showing three skyrmions. The PL signal is extracted along an elliptical contour of each skyrmion and plotted as a function of the angular position ϕ. Accumulation time per pixel 50 ms. (b) Extracted PL decrease along the contour of 19 skyrmions, black dots show the average value, with stronger noise around $\phi = 0$. (c)–(f) Expected noise distribution along the skyrmion contour for different skyrmion types. Thin colored lines are different disorder configurations, and black dots the mean value. In both the experiment and the calculations, the NV axis in-plane projection lies along $\phi = 0$.

perpendicularly magnetized films hosting a significant interfacial DMI.

Going a step further, we also studied skyrmions in SAF multilayers. Because DMI is critical for their existence, we anticipate that skyrmion noise maps can also provide signatures of the sign and strength of D. With the SAF sample shown in Fig. 2, skyrmions were nucleated by first applying an out-of-plane magnetic field of 220 mT subsequently lowered to 175 mT [29], after which the field is further reduced to a few mT. These skyrmions remain pinned at low fields and possess a diameter of about 200 nm, which appear as dark rings in the noise maps in Figs. 2(a) and 4(a). Interestingly, these dark rings do not exhibit a uniform PL intensity along their contours.

To better understand whether this nonuniformity is intrinsic to the internal spin texture or results only from disorder-related pinning, we compare the PL extracted along the contour of 19 skyrmions using an elliptical fitting function, as depicted in Fig. 4(a). We plot this data as a function of the angular position ϕ along the contour, with $\phi = 0$ corresponding to the horizontal direction on the images. Importantly, this horizontal direction corresponds to the in-plane projection of the NV axis, as determined by prior probe calibration. The resulting plots are shown in Fig. 4(b) as thin colored lines. While each curve exhibits large fluctuations, as a consequence of both the PL noise and the spatial disorder that distorts the shape of the skyrmion, averaging over the ensemble (black dots) reveals a clear trend where the PL decrease attains a maximum around $\phi = 0$.

We performed micromagnetic simulations of the magnetic noise in the SAF skyrmions following the method in Fig. 1. We assumed $d_{NV} = 50$ nm and considered 20 different realizations of magnetic disorder, comprising a 1% fluctuation in the perpendicular anisotropy, such that we obtain an ensemble of pinned skyrmions with diameters of about 200 nm but with varying shapes due to the disorder. This procedure was repeated for Bloch and Néel skyrmions with opposite chiralities. The calculated noise distributions are shown in Figs. 4(c)–4(f), with individual contours shown as thin colored lines and the average as black dots. Note that only the spatial component of the noise perpendicular to the NV axis contributes to the acceleration of the spin relaxation [12,33] and therefore to the noise contrast. This is the only element in the experiment breaking the circular symmetry, allowing the observation of specific noise patterns depending on the internal structure of the skyrmions. In agreement with the experimental data, we observe that a stronger noise level is expected around $\phi = 0$ (again the direction of the NV axis projection), resulting in the

maximum observed in the PL decrease in Fig. 4(b). We also notice that a significantly lower noise level is expected for Néel right than for Néel left skyrmions, similar to what occurs in domain walls, since it is again the in-plane magnetized region of the skyrmion boundary that contributes to the noise. The predicted variation for Bloch skyrmions is qualitatively different from the measured signal, consistent with the Néel configuration of the skyrmions.

We have shown that a combination of physical mechanisms allows insights into the sign and magnitude of DMI in thin films to be gleaned using scanning NV center microscopy. The asymmetric spin wave dispersion driven by the DMI, along with the wave-vector-dependent stray fields in thin films, produces magnetic noise associated with spin textures like domain walls and skyrmions that encodes the sign and strength of the DMI. This approach is especially useful in systems where standard inductive or optical techniques are inoperative, the spatial resolution of scanning NV center microscopy being crucial in order to exploit the signal from spin waves confined in nanoscale magnetic objects. It has the potential to be utilized for samples that produce moderate stray fields such as ferrimagnets, antiferromagnets, two-dimensional materials, and related van der Waals heterostructures, in order to determine the Bloch or Néel nature of skyrmions without the need for precise quantitative stray field measurements. Our findings unveil new possibilities for leveraging NV center microscopy not only for efficient characterization of magnetic materials but also for magnonics, as it provides access to the properties of spin waves confined within nanoscale magnetic textures, which are challenging to investigate using conventional tabletop experimental methods.

Acknowledgments—We acknowledge support from the European Union's Horizon 2020 research and innovation programme under Grants Agreements No. 964931 (TSAR) and No. 866267 (EXAFONIS).

Data availability—The data that support the findings of this Letter are openly available [46].

[1] N. A. Sinitsyn and Y. V. Pershin, The theory of spin noise spectroscopy: A review, Rep. Prog. Phys. **79**, 106501 (2016).

[2] M. Oestreich, M. Römer, R. J. Haug, and D. Hägele, Spin noise spectroscopy in GaAs, Phys. Rev. Lett. **95**, 216603 (2005).

[3] S. A. Crooker, J. Brandt, C. Sandfort, A. Greilich, D. R. Yakovlev, D. Reuter, A. D. Wieck, and M. Bayer, Spin noise of electrons and holes in self-assembled quantum dots, Phys. Rev. Lett. **104**, 036601 (2010).

[4] T. Jonsson, P. Nordblad, and P. Svedlindh, Dynamic study of dipole-dipole interaction effects in a magnetic nanoparticle system, Phys. Rev. B **57**, 497 (1998).

[5] B. C. Stipe, H. J. Mamin, T. D. Stowe, T. W. Kenny, and D. Rugar, Magnetic dissipation and fluctuations in individual nanomagnets measured by ultrasensitive cantilever magnetometry, Phys. Rev. Lett. **86**, 2874 (2001).

[6] J.-P. Tetienne, T. Hingant, L. Rondin, A. Cavaillès, L. Mayer, G. Dantelle, T. Gacoin, J. Wrachtrup, J.-F. Roch, and V. Jacques, Spin relaxometry of single nitrogen-vacancy defects in diamond nanocrystals for magnetic noise sensing, Phys. Rev. B **87**, 235436 (2013).

[7] D. Schmid-Lorch, T. Häberle, F. Reinhard, A. Zappe, M. Slota, L. Bogani, A. Finkler, and J. Wrachtrup, Relaxometry and dephasing imaging of superparamagnetic magnetite nanoparticles using a single qubit, Nano Lett. **15**, 4942 (2015).

[8] A. L. Balk, M. D. Stiles, and J. Unguris, Critical behavior of zero-field magnetic fluctuations in perpendicularly magnetized thin films, Phys. Rev. B **90**, 184404 (2014).

[9] T. van der Sar, F. Casola, R. Walsworth, and A. Yacoby, Nanometre-scale probing of spin waves using single electron spins, Nat. Commun. **6**, 7886 (2015).

[10] C. Du, T. van der Sar, T. X. Zhou, P. Upadhyaya, F. Casola, H. Zhang, M. C. Onbasli, C. A. Ross, R. L. Walsworth, Y. Tserkovnyak, and A. Yacoby, Control and local measurement of the spin chemical potential in a magnetic insulator, Science **357**, 195 (2017).

[11] H. Wang, S. Zhang, N. J. McLaughlin, B. Flebus, M. Huang, Y. Xiao, C. Liu, M. Wu, E. E. Fullerton, Y. Tserkovnyak, and C. R. Du, Noninvasive measurements of spin transport properties of an antiferromagnetic insulator, Sci. Adv. **8**, eabg8562 (2022).

[12] C. L. Degen, F. Reinhard, and P. Cappellaro, Quantum sensing, Rev. Mod. Phys. **89**, 035002 (2017).

[13] L. Rondin, J.-P. Tetienne, T. Hingant, J.-F. Roch, P. Maletinsky, and V. Jacques, Magnetometry with nitrogen-vacancy defects in diamond, Rep. Prog. Phys. **77**, 056503 (2014).

[14] A. Ariyaratne, D. Bluvstein, B. A. Myers, and A. C. B. Jayich, Nanoscale electrical conductivity imaging using a nitrogen-vacancy center in diamond, Nat. Commun. **9**, 2406 (2018).

[15] B. Flebus, H. Ochoa, P. Upadhyaya, and Y. Tserkovnyak, Proposal for dynamic imaging of antiferromagnetic domain wall via quantum-impurity relaxometry, Phys. Rev. B **98**, 180409(R) (2018).

[16] I. Dzyaloshinskii, Theory of helicoidal structures in antiferromagnets. I. Nonmetals, Sov. Phys. JETP **19**, 960 (1964).

[17] T. Moriya, Anisotropic superexchange interaction and weak ferromagnetism, Phys. Rev. **120**, 91 (1960).

[18] A. Finco, A. Haykal, R. Tanos, F. Fabre, S. Chouaieb, W. Akhtar, I. Robert-Philip, W. Legrand, F. Ajejas, K. Bouzehouane, N. Reyren, T. Devolder, J.-P. Adam, J.-V. Kim, V. Cros, and V. Jacques, Imaging non-collinear antiferromagnetic textures via single spin relaxometry, Nat. Commun. **12**, 767 (2021).

[19] A. Fert and P. M. Levy, Role of anisotropic exchange interactions in determining the properties of spin-glasses, Phys. Rev. Lett. **44**, 1538 (1980).

[20] A. Crépieux and C. Lacroix, Dzyaloshinsky–Moriya interactions induced by symmetry breaking at a surface, J. Magn. Magn. Mater. **182**, 341 (1998).

[21] M. Bode, M. Heide, K. von Bergmann, P. Ferriani, S. Heinze, G. Bihlmayer, A. Kubetzka, O. Pietzsch, S. Blügel, and R. Wiesendanger, Chiral magnetic order at surfaces driven by inversion asymmetry, Nature (London) **447**, 190 (2007).

[22] L. Udvardi and L. Szunyogh, Chiral asymmetry of the spin-wave spectra in ultrathin magnetic films, Phys. Rev. Lett. **102**, 207204 (2009).

[23] D. Cortés-Ortuño and P. Landeros, Influence of the Dzyaloshinskii–Moriya interaction on the spin-wave spectra of thin films, J. Phys. Condens. Matter **25**, 156001 (2013).

[24] J.-H. Moon, S.-M. Seo, K.-J. Lee, K.-W. Kim, J. Ryu, H.-W. Lee, R. D. McMichael, and M. D. Stiles, Spin-wave propagation in the presence of interfacial Dzyaloshinskii-Moriya interaction, Phys. Rev. B **88**, 184404 (2013).

[25] M. Kuepferling, A. Casiraghi, G. Soares, G. Durin, F. Garcia-Sanchez, L. Chen, C. H. Back, C. H. Marrows, S. Tacchi, and G. Carlotti, Measuring interfacial Dzyaloshinskii-Moriya interaction in ultrathin magnetic films, Rev. Mod. Phys. **95**, 015003 (2023).

[26] F. Garcia-Sanchez, P. Borys, R. Soucaille, J.-P. Adam, R. L. Stamps, and J.-V. Kim, Narrow magnonic waveguides based on domain walls, Phys. Rev. Lett. **114**, 247206 (2015).

[27] Y. Henry, D. Stoeffler, J.-V. Kim, and M. Bailleul, Unidirectional spin-wave channeling along magnetic domain walls of Bloch type, Phys. Rev. B **100**, 024416 (2019).

[28] See Supplemental Material at http://link.aps.org/supplemental/10.1103/dvbq-9z5f with additional data on a single ferromagnetic layer, calculations of the spin wave dispersion when varying D and of expected noise levels at different distances from the film, the preparation of the samples, the probe-to-sample distance calibrations, and details about the simulations, which includes Refs. [13,26,29–32].

[29] V. T. Pham, N. Sisodia, I. Di Manici, J. Urrestarazu-Larrañaga, K. Bairagi, J. Pelloux-Prayer, R. Guedas, L. D. Buda-Prejbeanu, S. Auffret, A. Locatelli, T. O. Menteş, S. Pizzini, P. Kumar, A. Finco, V. Jacques, G. Gaudin, and O. Boulle, Fast current-induced skyrmion motion in synthetic antiferromagnets, Science **384**, 307 (2024).

[30] T. Hingant, J.-P. Tetienne, L. J. Martínez, K. Garcia, D. Ravelosona, J.-F. Roch, and V. Jacques, Measuring the magnetic moment density in patterned ultrathin ferromagnets with submicrometer resolution, Phys. Rev. Appl. **4**, 014003 (2015).

[31] J. Leliaert, J. Mulkers, J. D. Clercq, A. Coene, M. Dvornik, and B. V. Waeyenberge, Adaptively time stepping the stochastic Landau-Lifshitz-Gilbert equation at nonzero temperature: Implementation and validation in MuMax 3, AIP Adv. **7**, 125010 (2017).

[32] A. Vansteenkiste, J. Leliaert, M. Dvornik, M. Helsen, F. García-Sánchez, and B. V. Waeyenberge, The design and verification of MuMax3, AIP Adv. **4**, 107133 (2014).

[33] M. Rollo, A. Finco, R. Tanos, F. Fabre, T. Devolder, I. Robert-Philip, and V. Jacques, Quantitative study of the response of a single NV defect in diamond to magnetic noise, Phys. Rev. B **103**, 235418 (2021).

[34] B. A. McCullian, A. M. Thabt, B. A. Gray, A. L. Melendez, M. S. Wolf, V. L. Safonov, D. V. Pelekhov, V. P. Bhallamudi, M. R. Page, and P. C. Hammel, Broadband multi-magnon relaxometry using a quantum spin sensor for high frequency ferromagnetic dynamics sensing, Nat. Commun. **11**, 5229 (2020).

[35] E. Lee-Wong, R. Xue, F. Ye, A. Kreisel, T. van der Sar, A. Yacoby, and C. R. Du, Nanoscale detection of magnon excitations with variable wavevectors through a quantum spin sensor, Nano Lett. **20**, 3284 (2020).

[36] I. Bertelli, J. J. Carmiggelt, T. Yu, B. G. Simon, C. C. Pothoven, G. E. W. Bauer, Y. M. Blanter, J. Aarts, and T. van der Sar, Magnetic resonance imaging of spin-wave transport and interference in a magnetic insulator, Sci. Adv. **6**, eabd3556 (2020).

[37] T. X. Zhou, J. J. Carmiggelt, L. M. Gächter, I. Esterlis, D. Sels, R. J. Stöhr, C. Du, D. Fernandez, J. F. Rodriguez-Nieva, F. Büttner, E. Demler, and A. Yacoby, A magnon scattering platform, Proc. Natl. Acad. Sci. U.S.A. **118**, e2019473118 (2021).

[38] I. Bertelli, B. G. Simon, T. Yu, J. Aarts, G. E. W. Bauer, Y. M. Blanter, and T. van der Sar, Imaging spin-wave damping underneath metals using electron spins in diamond, Adv. Quantum Technol. **4**, 2100094 (2021).

[39] B. G. Simon, S. Kurdi, J. J. Carmiggelt, M. Borst, A. J. Katan, and T. van der Sar, Filtering and imaging of frequency-degenerate spin waves using nanopositioning of a single-spin sensor, Nano Lett. **22**, 9198 (2022).

[40] C. Koerner, R. Dreyer, M. Wagener, N. Liebing, H. G. Bauer, and G. Woltersdorf, Frequency multiplication by collective nanoscale spin-wave dynamics, Science **375**, 1165 (2022).

[41] T. Devolder, Propagating-spin-wave spectroscopy using inductive antennas: Conditions for unidirectional energy flow, Phys. Rev. Appl. **20**, 054057 (2023).

[42] J. Mallinson, One-sided fluxes—A magnetic curiosity?, IEEE Trans. Magn. **9**, 678 (1973).

[43] A. Rustagi, I. Bertelli, T. van der Sar, and P. Upadhyaya, Sensing chiral magnetic noise via quantum impurity relaxometry, Phys. Rev. B **102**, 220403(R) (2020).

[44] W. Legrand, D. Maccariello, F. Ajejas, S. Collin, A. Vecchiola, K. Bouzehouane, N. Reyren, V. Cros, and A. Fert, Room-temperature stabilization of antiferromagnetic skyrmions in synthetic antiferromagnets, Nat. Mater. **19**, 34 (2020).

[45] J.-P. Tetienne, L. Rondin, P. Spinicelli, M. Chipaux, T. Debuisschert, J.-F. Roch, and V. Jacques, Magnetic-field-dependent photodynamics of single NV defects in diamond: An application to qualitative all-optical magnetic imaging, New J. Phys. **14**, 103033 (2012).

[46] A. Finco, P. Kumar, V. T. Pham, J. Urrestarazu-Larrañaga, R. Guedas García, M. Rollo, O. Boulle, J.-V. Kim, and V. Jacques, Thermal spin wave noise as a probe for the Dzyaloshinskii-Moriya interaction, 10.5281/zenodo.14808937 (2025).